



**HAL**  
open science

# Diverse roles and modulations of IA in spinal cord pain circuits

Nadine Clerc, Aziz Moqrich

► **To cite this version:**

Nadine Clerc, Aziz Moqrich. Diverse roles and modulations of IA in spinal cord pain circuits. Cell Reports, 2022, 38 (13), pp.110588. 10.1016/j.celrep.2022.110588 . hal-03871086

**HAL Id: hal-03871086**

**<https://cnrs.hal.science/hal-03871086>**

Submitted on 22 Jul 2024

**HAL** is a multi-disciplinary open access archive for the deposit and dissemination of scientific research documents, whether they are published or not. The documents may come from teaching and research institutions in France or abroad, or from public or private research centers.

L'archive ouverte pluridisciplinaire **HAL**, est destinée au dépôt et à la diffusion de documents scientifiques de niveau recherche, publiés ou non, émanant des établissements d'enseignement et de recherche français ou étrangers, des laboratoires publics ou privés.



Distributed under a Creative Commons Attribution - NonCommercial 4.0 International License

1 **Diverse roles and modulations of  $I_A$  in spinal cord pain circuits**

2

3 Nadine Clerc<sup>1,\*</sup> and Aziz Moqrich<sup>1</sup>

4

5 <sup>1</sup>Aix-Marseille-université, CNRS, Institut de Biologie du Développement de Marseille, UMR  
6 7288, case 907, 13288 Marseille Cedex 09, France.

7 Correspondance : [nadine.clerc@univ-amu.fr](mailto:nadine.clerc@univ-amu.fr)

8

9 **Summary**

10 **This review highlights recent findings of different amplitude ranges, roles and**  
11 **modulations of A-type  $K^+$  currents ( $I_A$ ) in excitatory (GAD67-GFP<sup>-</sup>) and inhibitory**  
12 **(GAD67-GFP<sup>+</sup>) interneurons in mouse spinal cord pain pathways. Endogenous**  
13 **neuropeptides, such as TFAFA4, oxytocin and dynorphin in particular, have been**  
14 **reported to modulate  $I_A$  in these pain pathways, but only TFAFA4 has been shown to**  
15 **reverse fully the opposing modulations that occur selectively in LIIo GAD67-GFP<sup>-</sup> and**  
16 **LIII GAD67-GFP<sup>+</sup> interneurons following both neuropathic and inflammatory pain. If,**  
17 **as hypothesized here, Kv4 subunits underlie  $I_A$  in both GAD67-GFP<sup>-</sup> and GAD67-GFP<sup>+</sup>**  
18 **interneurons, then  $I_A$  diversity in spinal cord pain pathways may depend on the**  
19 **interneuron subtype-selective expression of Kv4 auxiliary subunits with functionally**  
20 **different N-terminal variants. Thus,  $I_A$  emerges as a good candidate for explaining the**  
21 **mechanisms underlying injury-induced mechanical hypersensitivity.**

22

23

24

25

## 26 **Introduction**

27 A-type  $K^+$  currents ( $I_A$ ) were initially characterized in invertebrate neurons (Connor and  
28 Stevens, 1971a, b). They take their name from their typical profile generated by the opposing  
29 effects of fast activation and inactivation. Within the central nervous system and heterologous  
30 expression systems,  $I_A$  can be generated by multiple Kv pore-forming  $\alpha$  subunits: Kv1.4,  
31 Kv3.3, Kv3.4, all members of the Kv4 subfamily and Erg3 (Strube et al., 2015; Zemel et al.,  
32 2018). In addition, Kv1 subfamily  $\alpha$  subunits yielding delayed rectifier currents are rapidly  
33 inactivated when co-expressed with auxiliary  $\beta 1$  subunits (Jerng et al., 2004; Pongs and  
34 Schwarz, 2010).  $I_A$  can thus be generated by a wide variety of molecular entities with  
35 different gating and pharmacological properties, as summarized by (Zemel et al., 2018) and  
36 (Johnston, 2021).  $I_A$  is a low-voltage activating current when carried by Kv1.4 and Kv4s, but  
37 a high-voltage activating current when carried by Kv3.4. Recovery from inactivation is slow  
38 for  $I_A$  carried by Kv1.4 and Kv3.4, but fast for  $I_A$  carried by Kv3.3 and Kv4s. Remarkably, the  
39  $I_A$  carried by Kv4s has the most hyperpolarized voltage dependence for steady-state  
40 inactivation.

41 Native neuronal  $I_A$  ion channels function as macromolecular protein complexes including one  
42 or more Kv  $\alpha$  subunits (from a single subfamily) in association with cytosolic and/or  
43 transmembrane accessory subunits and regulatory proteins influencing channel stability,  
44 localization and biophysical properties. For example, for the  $I_A$  carried by Kv4  $\alpha$  subunits,  
45 two types of auxiliary subunits are classically described: Kv channel-interacting proteins  
46 (KChIPs) and dipeptidyl peptidase-like proteins (DPLPs). KChIPs are cytoplasmic calcium-  
47 binding proteins that interact with the intracellular moieties of the Kv4  $\alpha$  subunits, and DPLPs  
48 are type II transmembrane proteins (with a large extracellular portion) that associate with the  
49 Kv4 channel core (see (Pongs and Schwarz, 2010); (Jerng and Pfaffinger, 2014a). The roles of

50 the Kv  $\alpha$  subunits and I<sub>A</sub> channel accessory subunits depend on cell type (see (Carrasquillo  
51 and Nerbonne, 2014).

52 The roles of these different functional entities in dorsal root ganglion (DRG) neurons has  
53 recently been reviewed by (Zemel et al., 2018), and our understanding of the changes in I<sub>A</sub>  
54 channel expression, function and modulation in these neurons in pain models has progressed  
55 (Tsantoulas and McMahon, 2014; Zemel et al., 2018).

56 Fewer data are available for the spinal cord dorsal horn, but it is becoming clear that I<sub>A</sub> plays  
57 diverse roles in this structure. The spinal cord dorsal horn is a central nervous system  
58 structure divided into six Rexed laminae [with Lamina II (LII) subdivided into LII outer  
59 (LIIo) and inner (LIIi)] that receive the central terminals of primary afferent neurons and  
60 descending supraspinal projections (see (Moehring et al., 2018; Peirs and Seal, 2016; Todd,  
61 2010). It is, therefore, the principal site for primary afferent input integration and descending  
62 supraspinal modulation. Most C- and A $\delta$ - nociceptive primary afferents form synaptic  
63 contacts in the superficial laminae (LI and LII), whereas low-threshold A $\delta$ - and A $\beta$ -primary  
64 afferents mostly project onto deeper laminae (LIII to LV). At the border between LII and LIII,  
65 LIIi is the projection site of the low-threshold C- primary afferents, which are unusual in  
66 being able to transmit pleasant touch and modulate unpleasant mechanical pain sensations  
67 (Olausson et al., 2010; Seal et al., 2009; Yoo et al., 2021). The spinal cord dorsal horn  
68 includes a large number of excitatory and inhibitory interneuron populations (Abraira et al.,  
69 2017; Haring et al., 2018). LI and LII interneurons mostly respond to noxious peripheral  
70 stimulation, whereas the interneurons of deeper layers are more sensitive to touch. Projection  
71 neurons with cell bodies in LI and LIII transfer information to supraspinal sites, giving rise to  
72 the qualitative and affective aspects of pain sensation.

73 The gate control theory of pain was first proposed in 1965 (Melzack and Wall, 1965), and has  
74 evolved considerably since (Cui et al., 2016; Duan et al., 2014; Zhang et al., 2018). There is

75 now a consensus that lamina II neuron circuits play a major role in pain gating processes. (Hu  
76 et al., 2006), who used cultured mouse neurons from the LI to LIII laminae and pain models  
77 in mice (inflammation after carrageenan injection into the paw and chronic constriction of the  
78 sciatic nerve), were the first to put highlight on the importance of  $I_A$  in pain processing in the  
79 spinal cord dorsal horn. They identified Kv4.2  $\alpha$  subunits as crucial components by showing  
80 that the genetic elimination of this  $\alpha$  subunit decreased  $I_A$  and increased membrane  
81 excitability in cultured dorsal horn neurons. These features were correlated with enhanced  
82 sensitivity to tactile and thermal stimuli and were ERK-dependent.

83 Several studies based on patch clamp recordings on neurons in spinal cord slices have  
84 recently revealed an unexpected diversity of amplitude ranges, roles and modulations of  $I_A$  in  
85 LII pain pathways and the regulation of these modulations by endogenous neuropeptides with  
86 potential antinociceptive action. We provide here an overview of these recent advances and  
87 present some hypotheses that could be used as starting points for deciphering the cell and  
88 signaling pathways underlying these effects. Ionic current recording remains challenging in  
89 the spinal cord, and we, therefore, also consider ways in which it could be optimized.

### 90 **Optimizing $I_A$ resolution and isolation in the spinal cord in mouse models of pain**

91 Extensive data on  $I_A$  are lacking for spinal cord slices, probably because the spinal cord  
92 presents many obstacles to the accurate measurement of ionic currents. In particular, it  
93 becomes heavily myelinated and less resistant to anoxia during the first few weeks after birth,  
94 even though pain processes are immature at this point in development (see (Mitra and  
95 Brownstone, 2012). Each experimental step must be optimized to overcome these problems to  
96 make it possible to obtain data for the mature spinal cord (see Table 1). Alternatively, once  $I_A$   
97 pain-induced modulation has been observed in specific interneuron subtype using spinal cord  
98 slices, cultured neurons may be a more appropriate study model for deciphering cell signaling  
99 pathways, as they can bypass the obstacles specific to slices. Regardless of the study model

100 chosen, it is useful to begin by considering the situation from the viewpoint of the  
101 biophysicist, exploring the voltage dependence of the Kv channels at a large range of  
102 potentials. This generates useful information that can feed into physiological interpretations.  
103 The appropriateness of this strategy is illustrated by the fact that, for example, using a holding  
104 potential close to the resting membrane potential partly inactivates the  $I_A$  carried by Kv4  $\alpha$   
105 subunits (see above), which may prevent its detection, particularly if it is a small  $I_A$ .

### 106 **$I_A$ is expressed in excitatory and inhibitory dorsal horn interneurons**

107 Possible differences in  $I_A$  expression between the inhibitory and excitatory interneurons of the  
108 spinal cord dorsal horn have been investigated by patch-clamp recordings on interneurons  
109 from transgenic mice expressing enhanced GFP under the control of the promoter of the gene  
110 encoding the GABA-synthesizing enzyme GAD67 (GAD67-GFP<sup>+</sup> interneurons).  $I_A$  was  
111 recorded (with markedly different voltage protocols) with cultured neurons (Hu et al., 2006)  
112 or interneurons in spinal cord slices from young adult mice (Figure 1; (Yoo et al., 2021), the  
113 corresponding transgenic lines being generated by (Oliva et al., 2000) and (Tamamaki et al.,  
114 2003), respectively. In cultured neurons obtained from LI to LIII,  $I_A$  was induced with a +40  
115 mV step after a -80 mV conditioning prepulse (Hu and Gereau, 2011). In these conditions,  $I_A$   
116 densities were ~250 pA/pF in GAD67-GFP<sup>-</sup> neurons (excitatory neurons) and ~140 pA/pF in  
117 GAD67-GFP<sup>+</sup> neurons (inhibitory interneurons) which included a small percentage of  
118 neurons with no  $I_A$ . In interneurons recorded on slices,  $I_A$  was induced with a +70 mV step  
119 after a -120 mV conditioning prepulse (Yoo et al., 2021). With this protocol,  $I_A$  densities were  
120 determined for GAD67-GFP<sup>-</sup> and GAD67-GFP<sup>+</sup> interneurons selectively located in LIIIi or in  
121 LIIo. The values obtained were ~ 260 pA/pF for LIIIi GAD67-GFP<sup>-</sup> interneurons, ~295 pA/pF  
122 for LIIo GAD67-GFP<sup>-</sup> interneurons, ~40 pA/pF for LIIIi GAD67-GFP<sup>+</sup> interneurons and  
123 finally ~95 pA/pF for LIIo GAD67-GFP<sup>+</sup> interneurons. The data obtained when using the two  
124 different models were remarkably consistent leading to the conclusion that both types of

125 interneuron express  $I_A$  in naïve mice, but with striking differences in amplitude. Indeed, in  
126 GAD67-GFP<sup>-</sup> interneurons, which are excitatory, the  $I_A$  is large (see Figure 1); by contrast, in  
127 GAD67-GFP<sup>+</sup> interneurons, which are inhibitory, it is small (see Figure 1), sometimes at the  
128 limit of detection. The higher values obtained for cultured neurons than for neurons in slices  
129 probably reflect the possibility of recording ionic currents with lower access resistances ( $R_a$ )  
130 than in slices ( $R_a$ = 6-15 M $\Omega$  for cultured neurons in Hu and Gereau's study; (Hu and Gereau,  
131 2011) and  $\leq$  19 M $\Omega$  for neurons in slices in the study by (Yoo et al., 2021). See Table 1 for  
132 the consequences of high  $R_a$ .

133 The  $I_A$  in LII GAD67-GFP<sup>-</sup> interneurons is generally thought to be carried by Kv4.2  $\alpha$   
134 subunits (Hu et al., 2006; Hu and Gereau, 2011; Huang et al., 2005), but further investigations  
135 are required to identify unambiguously the ion channels carrying the  $I_A$  in LII GAD67-GFP<sup>+</sup>  
136 interneurons. After the off-line subtraction of  $I_{K_{DR}}$  from  $I_{K_{total}}$  on full current traces (see  
137 Table 1), the  $I_A$  in LII GAD67-GFP<sup>+</sup> interneurons typically displays fast inactivation (Figure  
138 1; (Yoo et al., 2021). (Yoo et al., 2021) systematically performed their recordings in the  
139 presence of a high TEA concentration to ensure that any current potentially carried by Kv3.3  
140 or Kv3.4 channels was blocked, due to the high TEA-sensitivity of these channels (see  
141 (Johnston, 2021; Strube et al., 2015). We can deduce that the  $I_A$  in LII GAD67-GFP<sup>+</sup>  
142 interneurons may be carried by Kv1.4 and/or Kv4s (probably Kv4.2 and Kv4.3) subunits.  
143 Kv1.4 immunoreactivity has been reported for neuronal soma from the rat dorsal horn  
144 (Edwards et al., 2002). If the  $I_A$  in GAD67-GFP<sup>+</sup> interneurons is carried largely by Kv1.4  
145 subunits it should recover slowly from inactivation (see (Johnston, 2021; Zemel et al., 2018).  
146 Remarkably, (Hu et al., 2006) found that most cultured GAD67-GFP<sup>+</sup> neurons were  
147 immunoreactive for Kv4.2. Less striking immunohistological staining results were obtained  
148 for slices. In particular, (Nowak et al., 2011) detected no immunoreactivity for either Kv4.2 or  
149 Kv4.3 in the soma of GAD67-GFP<sup>+</sup> interneurons. These negative results may reflect

150 immunostaining for Kv4s being below the threshold of detection at the cell body membrane,  
151 but stronger in neuronal processes. Consistent with this hypothesis, (Huang et al., 2005)  
152 detected Kv4.2 immunoreactivity in “long fibrous structures extending rostro caudally” and  
153 reminiscent of the processes of islet cells (which are exclusively inhibitory) but never in  
154 neuronal cell bodies in rats. (Strube et al., 2015) were also unable to visualize Kv4-  
155 immunoreactive neuronal cell bodies in the nucleus of the tractus solitarius of the Rat, even  
156 though AmmTX3, a scorpion toxin of the  $\alpha$ -KTX 15 family that blocks all Kv4s, inhibited  $I_A$   
157 by 80% in this structure. To unambiguously demonstrate that, as suspected, the  $I_A$  in GAD67-  
158 GFP<sup>+</sup> LIII interneurons is mainly carried by Kv4s, similar pharmacological experiments  
159 should be performed on these interneurons, possibly after SNI to get relatively high  $I_A$  control  
160 values.

### 161 **In neuropathic and inflammatory pain, $I_A$ is modulated differentially in excitatory and** 162 **inhibitory dorsal horn interneurons**

163 The induction of irreversible neuropathic pain by spared nerve injury (SNI) in gad1<sup>GFP</sup> mice  
164 leads to an upregulation of  $I_A$  in LIII GAD67-GFP<sup>+</sup> interneurons and a downregulation of this  
165 current in LIIo GAD67-GFP<sup>-</sup> interneurons (Table 2; (Tamamaki et al., 2003; Yoo et al.,  
166 2021). Interestingly,  $I_A$  is unaffected in LIIo GAD67-GFP<sup>+</sup> interneurons and in LIII GAD67-  
167 GFP<sup>-</sup> interneurons. The increase in  $I_A$  reached 74% of control values for  $I_A$  evoked by  
168 depolarizing steps of +70 mV after a -120 mV conditioning prepulse, in LIII GAD67-GFP<sup>+</sup>  
169 interneurons (Table 2) and the  $I_A$  in LIIo GAD67-GFP<sup>-</sup> interneurons was about 35% lower  
170 than control values (Table 2). A decrease in  $I_A$  has also been observed in LIIo excitatory  
171 interneurons (particularly LIIo SOM<sup>Cre</sup>-negative interneurons) during inflammation induced  
172 by capsaicin injection into the hind paw (Zhang et al., 2018). (Harris et al., 2014) described a  
173 similar effect in the upper cervical superficial dorsal horn neurons following acute neck  
174 muscle inflammation due to carrageenan injection. These neurons were blindly patched and

175 were not, therefore, functionally identified, but it can be inferred that they were excitatory.  
176 Indeed, in these neurons,  $I_A$  was evoked by the application of a low depolarizing voltage  
177 (from -90 to -40 mV), which would have been much too low to produce a detectable  $I_A$  in LIII  
178 GAD67-GFP<sup>+</sup> interneurons, or even LIIo GAD67-GFP<sup>+</sup> interneurons (Yoo et al., 2021).  
179 Overall, these data suggest that, in mice, LII interneurons are sensitized, during both  
180 neuropathic and inflammatory pain, by opposing modulations of  $I_A$  in LIII inhibitory and LIIo  
181 excitatory interneurons. The role of  $I_A$  therefore differs between these two interneuron  
182 subpopulations.

183  **$I_A$  has opposite roles in LIIo excitatory and LIII inhibitory interneurons, in both the**  
184 **presence and absence of pain**

185 In LIII inhibitory interneurons in naïve conditions, a small  $I_A$  should lead to high levels of  
186 neuron excitability, consistent with reports of mostly tonic firing in GAD67-GFP<sup>+</sup> or GAD65-  
187 GFP<sup>+</sup> interneurons (Cui et al., 2011; Daniele and MacDermott, 2009; Punnakkal et al., 2014;  
188 Zhang and Dougherty, 2011). A similar firing pattern has been reported for LIII  
189 subpopulations of inhibitory neurons, such as glycinergic (GLY) interneurons expressing  
190 dynorphin (DYN<sup>+</sup>; (Duan et al., 2014) or parvalbumin positive (PV<sup>+</sup>) interneurons (Boyle et  
191 al., 2019). A much larger  $I_A$  after SNI probably results in lower rates of neuron firing.  
192 Consistent with this theoretical assumption, the excitability of PV<sup>+</sup> interneurons decreases  
193 after SNI (Boyle et al., 2019). More specifically, the amplitude of the current injection  
194 required to maintain tonic firing increased after SNI. PV<sup>+</sup> interneurons, with their islet cell-  
195 like morphology, are typified by a hyperpolarization-activated current ( $I_h$ ; (Boyle et al., 2019;  
196 Hughes et al., 2012) carried by HCN channels and known to act in opposition to  $I_A$  (see (Biel  
197 et al., 2009). This is also a characteristic of the wider population of LIII GAD67-GFP<sup>+</sup>  
198 interneurons, which present a large  $I_h$  in naïve conditions (Yoo et al., 2021). Yoo et al. (2021)  
199 reported a large decrease in this  $I_h$  after SNI, whereas (Boyle et al., 2019) reported no change.

200 This discrepancy can be explained by the restriction of the SNI-induced effect reported by  
201 (Yoo et al., 2021) to the interneurons located in the circumscribed area of SNI-induced  
202 microglial activation, rendering its detection unlikely when interneurons are sampled from a  
203 larger area ipsilateral to SNI (Boyle et al., 2019). In conclusion, through opposite effects on  $I_A$   
204 and  $I_h$ , (increasing  $I_A$  and decreasing  $I_h$ ), SNI generates synergistic modulations of  $I_A$  and  $I_h$   
205 leading to a strong decrease in the excitability of LIIi inhibitory interneurons.

206 In LIIo excitatory interneurons, a large  $I_A$  is required to decrease excitability in naïve  
207 conditions. This is illustrated by LIIo SOM<sup>Cre</sup>-negative interneurons, in which  $I_A$  strongly  
208 delays the action potential firing triggered by depolarizing steps. As expected, this delay is  
209 abolished when  $I_A$  is blocked with 4-AP (Zhang et al., 2018) and should be reduced after SNI  
210 decreasing  $I_A$  by one third in GAD67-GAD<sup>-</sup> interneurons (Yoo et al., 2021).

211 LIIi GAD67-GFP<sup>+</sup> interneurons display modulations of  $I_A$  (and  $I_h$ ) that cannot be generalized  
212 to their LIIo counterpart. In naïve conditions, these LIIo interneurons have a large  $I_A$  (albeit  
213 much smaller than that in LIIo GAD67-GFP<sup>-</sup> interneurons; see Figure 1) and a very small  $I_h$ .  
214 SNI does not significantly modify either of these currents in the total LIIo GAD-GFP<sup>-</sup>  
215 interneuron population (Yoo et al., 2021).

216  $I_A$  modulation is not a general feature of all GAD67-GFP<sup>-</sup> interneurons.  $I_A$  and  $I_h$  have large  
217 amplitudes in LIIi and LIIo GAD67-GFP<sup>-</sup> interneurons in control conditions (see Fig. 1), but  
218 SNI modulates  $I_A$  only in LIIo neurons after SNI, with  $I_h$  remaining unaffected in all GAD67-  
219 GFP<sup>-</sup> interneuron subtypes.

220 The selectivity of  $I_A$  and  $I_h$  modulations between different subtypes of interneuron at strategic  
221 locations within LII probably reflects specific functions of  $I_A$  and  $I_h$  in pain gate control  
222 circuits.

223 **Functional role of  $I_A$  modulations in pain gate control circuits**

224 In the pain gate control circuits,  $I_A$  function differs between interneuron types (Figure 2). In  
225 LIIo excitatory interneurons, particularly those that transmit pain [the T neurons of the gate  
226 control theory; see (Duan et al., 2014) and (Zhang et al., 2018)],  $I_A$  establishes permissive  
227 conditions for feed-forward inhibition, whereas, in LIIIi inhibitory interneurons, it modulates  
228 the feed-forward inhibition capacity.

229 As elegantly demonstrated by (Zhang et al., 2018), the  $I_A$  in LIIo acts as an electric filter  
230 operating in LIIo  $SOM^{Cre}$  negative interneurons, a subtype of excitatory interneurons acting as  
231 T neurons. In these interneurons, when  $I_A$  is large (in naïve conditions), most attempts to  
232 stimulate  $A\beta$  fibers fail to produce action potentials, reflecting the closed configuration of the  
233 gate (Figure 2; left panel). By contrast, when the  $I_A$  in these interneurons is blocked with  
234 intracellular 4-AP (in the absence of the sensitization of other gate-control circuit elements),  
235 most stimulations of  $A\beta$  fibers generate action potentials, indicating that the gate is open. A  
236 similar effect is observed when  $I_A$  in these interneurons is decreased due to the sensitization  
237 (expressed by mechanical hypersensitivity) following the injection of capsaicin into mouse  
238 hind paw (Zhang et al., 2018). It likely also occurs after  $I_A$  decrease in LIIo  $GAD67-GFP^-$   
239 interneurons following SNI (Yoo et al. 2021; Figure 2).

240 The  $I_A$  in LIIo excitatory interneurons may be large due to a constitutive release of dynorphin  
241 (DYN). This hypothesis emerged from observations of a decrease in  $I_A$  in LIIo excitatory  
242 interneurons (in particular LIIo  $SOM^{Cre}$ -negative interneurons) in conditions in which DYN  
243 release is suppressed by the genetic ablation of  $DYN^+$  interneurons (Zhang et al., 2018).  
244 According to this hypothesis, DYN release should decrease,  $I_A$  should increase and action  
245 potential firing should decrease in LIIo  $DYN^+ GLYT2^-$  interneurons (the most abundant  
246 DYN-positive neurons in LIIo), following the lesioning of nerves or inflammation. However,  
247 as Zhang et al. (2018) did not selectively manipulate DYN signaling but ablated the entire  
248 DYN neuronal population,  $I_A$  expression might be regulated by other factors released from

249 DYN neurons or by indirect consequences of widespread cell death within the dorsal horn  
250 following the ablation. In addition, the fact that, in GAD67-GFP<sup>-</sup> interneurons, I<sub>A</sub> is large in  
251 both slices and cultures (see above), suggests that this current is shaped by intrinsic factors in  
252 these interneurons.

253 Another set of DYN<sup>+</sup> interneurons, the LIIi DYN<sup>+</sup> GLYT2<sup>+</sup> interneurons located at the  
254 LII/LIII border and thus included in the LIIi GAD67-GFP<sup>+</sup> interneuron population, may also  
255 have an important function. Indeed, in this area of the dorsal horn, the number of interneurons  
256 generating A $\beta$ -evoked action potentials increases considerably following genetic ablation of  
257 the entire DYN<sup>+</sup> interneuron population (Zhang et al., 2018). These LIIi DYN<sup>+</sup> GLYT2<sup>+</sup>  
258 interneurons may not display a change in I<sub>h</sub> (this current being known to be substantial only in  
259 PV<sup>+</sup> interneurons), but they could be involved in the increase in I<sub>A</sub> observed in LIIi GAD67-  
260 GFP<sup>+</sup> interneurons after SNI (Yoo et al., 2021). Finally, within the population of LIIi GAD67-  
261 GFP<sup>+</sup> interneuron population, the PV<sup>+</sup> interneurons are the most likely to display an increase  
262 in I<sub>A</sub> accompanied by a decrease in I<sub>h</sub> after SNI (Yoo et al., 2021). As indicated above, these  
263 patterns of I<sub>A</sub> and I<sub>h</sub> modulations in LIIi GAD67-GFP<sup>+</sup> interneurons should markedly reduce  
264 their electrical activity, and, thus, their classical inhibitory function via inhibitory postsynaptic  
265 potentials and currents. This inhibition probably has multiple consequences, as LIIi DYN<sup>+</sup>  
266 GLYT2<sup>+</sup> interneurons are subject to feed-forward inhibition (Duan et al., 2014), whereas PV<sup>+</sup>  
267 interneurons target several populations of LII interneurons (Boyle et al., 2019) and have been  
268 reported to inhibit A $\beta$  terminals presynaptically (Boyle et al., 2019).

### 269 **Endogenous peptides with potential antinociceptive action via I<sub>A</sub> modulation in LII**

270 Numerous endogenous pain modulators (opioids, nociceptin, cannabinoids, adenosine,  
271 adenosine 5'-triphosphate (ATP), bradykinin, norepinephrine, serotonin, dopamine,  
272 somatostatin, galanin, substance P, neuropeptide Y, oxytocin and acetylcholine) have been  
273 shown to induce changes in excitatory or inhibitory synaptic transmission and membrane

274 potential in the spinal lamina II interneurons. The targets on which these endogenous  
275 analgesics act are mostly membrane proteins, such as receptors for neurotransmitters or the  
276 potassium-chloride exporter KCC2 [see (Kumamoto, 2019) for review]. As mentioned above,  
277 DYN could potentially constitutively upregulate  $I_A$  in LIIo  $SOM^{Cre}$ -negative interneurons, but  
278 the only other modulator reported to act on  $I_A$  in LII interneurons is oxytocin, a peptide  
279 released by axons originating from a neuron subpopulation of the paraventricular nucleus of  
280 the hypothalamus (PVN) and terminating in superficial layers of the spinal cord (Breton et al.,  
281 2009). Another recently discovered potential endogenous analgesic, TAF4, a neuropeptide  
282 produced by C-LTMRs, has been shown to act through the differential modulation of  $I_A$  in  
283 LIIo  $GAD67-GFP^-$  and LIII  $GAD67-GFP^+$  interneurons (Yoo et al., 2021).

284 Oxytocin -whether secreted in the spinal cord after PVN stimulation applied or exogenously  
285 by intrathecal infusion- has been shown to have antinociceptive properties during the  
286 development of inflammatory or neuropathic pain [see (Breton et al., 2009; Kumamoto,  
287 2019). A study based on patch-clamp recordings of blindly patched neurons in rat spinal cord  
288 slices showed that bath applications of the specific oxytocin receptor agonist TGOT decreased  
289  $I_A$  and  $IK_{DR}$  respectively by 45% and 42%, in LII interneurons. These down regulations of  
290 potassium currents synergically decreased the firing ability of LII interneurons, specifically  
291 those with bursting firing patterns (Breton et al., 2009). In mice, oxytocin receptor-expressing  
292 interneurons are always immunoreactive for ChAT (and may therefore be considered  
293 probably excitatory) and have been reported to be interspersed with protein kinase  $C\gamma$   
294 interneurons in LIII (Wrobel et al., 2011). Further studies are required to determine whether  $I_A$   
295 is modulated in these ChAT positive interneurons in conditions of neuropathic pain and  
296 whether this modulation is reversed by oxytocin.

297 TAF4 is produced by C-LTMRs. In control conditions, TAF4-containing central terminals  
298 project onto LIII, below the  $PKC\gamma$ -positive interneurons, with peripheral terminals innervating

299 the hair follicles in the dermis (Delfini et al., 2013; Hoeffel et al., 2021; Yoo et al., 2021). In  
300 the skin sunburn model, skin damage induces an increase in TAFA4 production by DRGs  
301 leading to an increase in TAFA4 levels in the skin. This increase triggers a dysregulation of  
302 macrophage activity leading to an increase in the concentration of IL-10, which has anti-  
303 inflammatory effects, ultimately favoring skin repair (Hoeffel et al., 2021). No data are  
304 currently available concerning putative changes in TAFA4 production within the dorsal spinal  
305 cord after peripheral inflammation or sciatic nerve injury. After SNI, TAFA4 persists in the  
306 projection territory of the spared C-LTMRs but disappears from the spinal territory displaying  
307 strong microglial activation.  $I_A$  (together with  $I_h$ ) has been shown to be modulated in specific  
308 populations of interneurons within this highly perturbed area, as described above (Yoo et al.  
309 2021). Each SNI-induced modulation can be reversed by incubating the spinal cord slices in  
310 an external solution containing TAFA4. In other words, the exogenous administration of  
311 TAFA4 results in opposite modulations of  $I_A$  in LIIo GAD67-GFP<sup>-</sup> and LIIIi GAD67-GFP<sup>+</sup>  
312 interneurons (increasing and decreasing  $I_A$ , respectively). These modulations can be prevented  
313 by adding RAP (receptor-associated protein), an LDL-receptor antagonist, together with  
314 TAFA4. In parallel, TAFA4 reversed inflammatory, postoperative and SNI-induced  
315 mechanical hypersensitivity in both male and female mice, also in an LDL receptor-dependent  
316 manner (Yoo et al., 2021).

317 How does the exogenous administration of TAFA4 lead to opposite changes in  $I_A$  in LIIo  
318 GAD67-GFP<sup>-</sup> and LIIIi GAD67-GFP<sup>+</sup> interneurons? Several scenarios are possible:

319 (i) TAFA4 may activate different cellular and/or molecular pathways independently targeting  
320  $I_A$  in LIIo GAD67-GFP<sup>-</sup> and in LIIIi GAD67-GFP<sup>+</sup> interneurons. For example, both neuronal  
321 and non-neuronal sources of reactive oxygen and nitrogen (nitroxidative) species (ROS and  
322 RNS) implicated in pain processing (Grace et al., 2016; Jerng and Pfaffinger, 2014b;  
323 Kuboyama et al., 2011) might be involved. In this scenario, TAFA4 may act by decreasing the

324 production of ROS and RNS, consistent with the recently described anti-inflammatory  
325 function of this molecule (Hoeffel et al., 2021). Following SNI, the elimination of TFAFA4  
326 from the central terminals of the cut C-LTMRs probably contributes to the irreversibility of  
327 pain, and only exogenous TFAFA4 is effective in this context. ROS increase  $I_A$  only when this  
328 current is produced by Kv4 channels complexed with DPLP6a and/or DPLP10a (Jerng and  
329 Pfaffinger, 2014a, b). It therefore seems possible that, after SNI, ROS increase  $I_A$  in LIII  
330 GAD67-GFP<sup>+</sup> interneurons but not in LIIo GAD67-GFP<sup>-</sup> interneurons, based on the  
331 assumption that DPLP6a and/or DPP10a are expressed in the former but not the latter.  
332 Interestingly, in the dorsal horn of the spinal cord, the expression of DPPL6 and DPPL10 is  
333 heterogeneous as most LI, LIII and LV dorsal horn projection neuron express DPPL10  
334 whereas LII neurons express a strong DPPL6 immunoreactivity colocalized with Kv4.2 and  
335 KChiP2 in rostrocaudal dendrites (Cheng et al., 2016). However, the DPLP6 paralog  
336 subdistribution has not been determined and it remains unknown whether these rostrocaudal  
337 dendrites emerge from islet cells (inhibitory neurons), as might be expected. A simple way of  
338 testing the relevance of this hypothesis would be to check, in naive GAD67 mice, whether the  
339 small  $I_A$  in LIII GAD67-GFP<sup>+</sup> interneurons increases following addition of the highly  
340 membrane-permeant H<sub>2</sub>O<sub>2</sub> analog tert-butyl hydroperoxide (see (Jerng and Pfaffinger, 2014a).  
341 If this is indeed the case, then another modulator would be expected to act on LIIo GAD67-  
342 GFP<sup>-</sup> interneurons to trigger a decrease in  $I_A$ . At least in the heart,  $I_A$  ( $I_{to}$ , carried by Kv4.3) is  
343 downregulated by NO (Fernandez-Velasco et al., 2007; Gomez et al., 2008). For  $I_h$  in LIII  
344 GAD67-GFP<sup>+</sup> interneurons, the activity of HCN channels has also been shown to be  
345 downregulated by NO, via a mechanism known as S-nitrosylation (see (Pires da Silva et al.,  
346 2016).

347 (ii) Alternatively, a single cellular and molecular pathway (summarized in figure 2) may be  
348 involved. In the SNI model, exogenous TFAFA4 may preferentially target LIII GAD67-GFP<sup>+</sup>

349 interneurons, the activity of which modulates  $I_A$  levels in LIIo GAD67-GFP<sup>-</sup> interneurons. As  
350 suggested above, the activity of LIII DYN<sup>+</sup>GLYT2<sup>+</sup> interneurons and LIII PV<sup>+</sup> interneurons  
351 may decrease after SNI, subsequently being restored by TAF4, which would enable the LIIo  
352 GAD67-GFP<sup>-</sup> interneurons to recover their initial  $I_A$  amplitude.

353 This second scenario potentially works with any A-type channel  $\alpha$  subunit. It implies that  $I_A$   
354 and  $I_h$ , in LIII GAD67-GFP<sup>+</sup> and LIIo GAD67-GFP<sup>-</sup> interneurons involved in a specific  
355 pathway, are modulated by neurotransmitters acting in (or controlling) these pathways. The  
356 first scenario requires the expression of specific Kv4 ternary complexes in LIII GAD67-GFP<sup>+</sup>  
357 and LIIo GAD67-GFP<sup>-</sup> interneurons. Whatever the LII pain pathways including these  
358 interneurons and the identity of the involved neurotransmitters,  $I_A$  and  $I_h$  modulations are  
359 conditioned by ROS or RNS acting on “adequat” Kv4 ternary complexes.

### 360 **Concluding remarks**

361 In the spinal cord dorsal horn, the amplitude range and role of  $I_A$  and its modulation after  
362 sensitization due to inflammation or nerve lesions differ considerably between interneuron  
363 subpopulations (as shown for LIIo GAD67-GFP<sup>-</sup> and LIII GAD-67GFP<sup>+</sup> interneurons). The  
364 pathological consequences of perturbations of the intrinsic properties of spinal cord dorsal  
365 horn interneurons remain underestimated, but they could, as described here, play a major role  
366 in pain plasticity.

367 Endogenous neuropeptides, such as TAF4, oxytocin and DYN in particular, have been  
368 reported to modulate  $I_A$ . In naïve conditions, oxytocin and DYN may have opposite effects,  
369 probably on different excitatory interneuron subtypes. However, it remains unclear whether  
370 these neuropeptides act in pain conditions. TAF4 is the only one of these neuropeptides for  
371 which an effect has been shown in pain conditions. It has been shown to reverse pain-induced  
372 alterations of  $I_A$  in both excitatory and inhibitory interneurons (specifically in LIIo GAD67-  
373 GFP<sup>-</sup> and LIII GAD-67-GFP<sup>+</sup> interneurons).

374 Further studies will be required to determine the biophysical properties, molecular  
375 determinants, modulation mechanisms and functional roles of  $I_A$  in spinal cord pain circuits.  
376 For this, it will be probably useful to refine the identification of the LII GAD67-GFP<sup>+</sup> and  
377 GAD67-GFP<sup>-</sup> interneurons that display pain-induced  $I_A$  modulations, and to focus on the  
378 interneuron subtypes for which deletions affect gating processes in the spinal cord dorsal  
379 horn. In the case of the GAD67-GFP<sup>+</sup> interneuron population, PV<sup>+</sup> and DYN<sup>+</sup> interneurons  
380 fulfil this criterion (see (Cui et al., 2016; Duan et al., 2014; Petitjean et al., 2015). PV<sup>+</sup>  
381 interneurons, which characteristically have a large  $I_h$ , probably account for a large proportion  
382 of the LIII GAD67-GFP<sup>+</sup> interneurons displaying alterations of both  $I_A$  and  $I_h$  after SNI (Yoo  
383 et al., 2021). It remains unclear whether pain-induced modulations of  $I_A$  also occur in DYN<sup>+</sup>  
384 neurons. In addition, deep layer (LIII-V) inhibitory neurons that express the receptor tyrosine  
385 kinase Ret neonatally might be targeted as they mediate crosstalk between touch and pain  
386 pathways (Cui et al., 2016).

387 The LII GAD67-GFP<sup>-</sup> interneuron population contains numerous subpopulations of cells with  
388 a uniformly large  $I_A$  (Hu and Gereau, 2011; Yoo et al., 2021). The relatively large SOM<sup>Cre</sup>-  
389 derived neuron population is essential for the expression of mechanical hypersensitivity  
390 (Cheng et al., 2017; Zhang et al., 2018), and might thus include some neuron subpopulations  
391 with pain-induced modulations of  $I_A$ . However, studies to date have focused on LIIo SOM<sup>Cre</sup>-  
392 negative interneurons (not yet identified) because, unlike SOM<sup>Cre</sup>-derived neurons, these cells  
393 receive frequent A $\beta$  evoked action potentials after capsaicin treatment, due to  $I_A$  decrease in  
394 these neurons (Zhang et al., 2018).

395 If the pain-modulated  $I_A$  is carried by Kv4s in GAD67-GFP<sup>+</sup> interneurons as in GAD67-GFP<sup>-</sup>  
396 interneurons, then its functional diversity likely reflects that of the components of the full  
397 ternary complex Kv4-KChIP-DPLP (coupled to T and L Ca<sub>v</sub> channels; see (Anderson et al.,  
398 2013; Jerng and Pfaffinger, 2014a)). These components should thus be identified in each

399 interneuron subtype exhibiting pain-modulated I<sub>A</sub> because the expression of the different Kv4  
400 auxiliary subunit paralogs is neuron specific; such knowledge should make it possible to  
401 develop novel targeted therapeutics as stated by Jerng and Pfaffinger (2014a).  
402 Concerning the mechanisms of I<sub>A</sub> modulation, the ERK-signaling-dependent downregulation  
403 of I<sub>A</sub>, which was first described in superficial dorsal horn interneurons at the beginning of the  
404 21<sup>st</sup> century (Hu et al., 2006; Hu and Gereau, 2003; Hu et al., 2003), is now known to occur in  
405 some LIIo excitatory interneurons (Zhang et al., 2018). Different, as yet, undetermined  
406 signaling processes probably occur in LIII GAD67-GFP<sup>+</sup> interneurons to mediate the opposite  
407 patterns of I<sub>A</sub> modulation reported by Yoo et al (2021).  
408 Thus, the diversity of I<sub>A</sub> amplitude ranges, roles and modulations highlighted in this review  
409 are probably dependent on interneuron subtype selectivity of expression of a large range of  
410 molecular substrates (Cav-Kv4 complex) and multiple signaling pathways.

411

## 412 **ACKNOWLEDGMENTS**

413

414 This work was funded by the French National Research Agency (ANR-CE16-Myochronic  
415 grant) and by the "Fondation pour la Recherche Médicale (FRM)" Equipe FRM-  
416 EQP202003010192, grants awarded to AM. This work was also supported by institutional  
417 funding from the CNRS and Aix-Marseille-Université awarded to IBDM.

## 418 **AUTHOR CONTRIBUTIONS**

419 N.C was responsible for performing the literature review and writing the article. A.M made  
420 substantial contributions to discussions concerning the content of the review article.

## 421 **DECLARATION OF INTEREST**

422 The authors have no competing interest to declare.

423

424

425

426

## 427 **FIGURE LEGENDS**

### 428 **Figure 1: I<sub>A</sub> in laminae IIo and III GAD67-GFP-positive and -negative interneurons in** 429 **spinal slices**

430 I<sub>A</sub> (blue or purple traces) was evoked by a +70 mV step (as shown in the central panel) and  
431 isolated by off-line subtraction [(**Total IK at +70 mV from -120 mV**) - (**IK<sub>DR</sub> at +70mV**  
432 **from -30 mV**)]. Note that GAD67-GFP<sup>+</sup> LIII interneurons had a large IK<sub>DR</sub>, as previously  
433 described by Hu & Gereau (2011) in cultured neurons. The arrowhead before the red trace on  
434 the right indicates that, in LIII GAD67-GFP<sup>+</sup> interneurons in naïve conditions, I<sub>A</sub> was  
435 preceded by a hyperpolarizing activated inward current (I<sub>h</sub>) evoked by the -120 mV prepulse  
436 (see Yoo et al. 2021; Fig 4B and 5B). The same scaling was used for all current traces.

### 437 **Figure 2: I<sub>A</sub> and I<sub>h</sub> modulations in LII interneurons after SNI or inflammation**

438 In control conditions (left panel), a large I<sub>A</sub> in LIIo excitatory interneuron (probably vertical  
439 cells and possibly SOM<sup>Cre</sup>-negative interneurons; white with black plus) allows these neurons  
440 to gate A $\beta$ -LTMR inputs (Zhang et al. 2018) and to prevent the activation of the mechanical  
441 pain pathway (doted vertical arrow). Such a large I<sub>A</sub> in LIIo excitatory interneurons might  
442 depend (oblique dote arrow) on the LIII inhibitory interneuron intense firing favored by a  
443 small I<sub>A</sub> and a large I<sub>h</sub>. These LIII inhibitory interneurons (black with white minus) might be  
444 PARV<sup>+</sup> interneurons possibly also generating feed-forward inhibition onto LIII DYN<sup>+</sup>  
445 GLYT2<sup>+</sup> interneurons and synaptically connected to vertical cells (Boyle et al. 2019). After  
446 nerve lesion such as SNI (right panel), LIII inhibitory neurons lose their braking activity as I<sub>A</sub>  
447 decreases and I<sub>h</sub> increases with, as a final consequence, a decrease in I<sub>A</sub> in LIIo excitatory  
448 interneurons that thus lose their gating ability as shown by Zhang et al. (2018). In these  
449 conditions, the mechanical pain pathway is activated (black vertical arrow).

450 The stylized traces are based on data from Zhang et al. (2018) and Yoo et al. (2021) for LIIo  
451 excitatory interneurons and exclusively from Yoo et al. (2021) for LIII inhibitory  
452 interneurons.

453 The one \* means that the data were exclusively obtained by Yoo et al. (2021). The two \*\*  
454 means that the data obtained by Yoo et al. (2021) were the same as those obtained by Zhang  
455 et al. (2018).

## 456 **References**

- 457 Abraira, V.E., Kuehn, E.D., Chirila, A.M., Springel, M.W., Toliver, A.A., Zimmerman, A.L., Orefice, L.L.,  
458 Boyle, K.A., Bai, L., Song, B.J., *et al.* (2017). The Cellular and Synaptic Architecture of the  
459 Mechanosensory Dorsal Horn. *Cell* 168, 295-310 e219.
- 460 Anderson, D., Engbers, J.D., Heath, N.C., Bartoletti, T.M., Mehaffey, W.H., Zamponi, G.W., and  
461 Turner, R.W. (2013). The Cav3-Kv4 complex acts as a calcium sensor to maintain inhibitory charge  
462 transfer during extracellular calcium fluctuations. *J Neurosci* 33, 7811-7824.
- 463 Biel, M., Wahl-Schott, C., Michalakis, S., and Zong, X. (2009). Hyperpolarization-activated cation  
464 channels: from genes to function. *Physiol Rev* 89, 847-885.
- 465 Boyle, K.A., Gradwell, M.A., Yasaka, T., Dickie, A.C., Polgar, E., Ganley, R.P., Orr, D.P.H., Watanabe,  
466 M., Abraira, V.E., Kuehn, E.D., *et al.* (2019). Defining a Spinal Microcircuit that Gates Myelinated  
467 Afferent Input: Implications for Tactile Allodynia. *Cell reports* 28, 526-540 e526.
- 468 Breton, J.D., Poisbeau, P., and Darbon, P. (2009). Antinociceptive action of oxytocin involves  
469 inhibition of potassium channel currents in lamina II neurons of the rat spinal cord. *Mol Pain* 5, 63.
- 470 Carrasquillo, Y., and Nerbonne, J.M. (2014). IA channels: diverse regulatory mechanisms.  
471 *Neuroscientist* 20, 104-111.
- 472 Cheng, C.F., Wang, W.C., Huang, C.Y., Du, P.H., Yang, J.H., and Tsaur, M.L. (2016). Coexpression of  
473 auxiliary subunits KChIP and DPPL in potassium channel Kv4-positive nociceptors and pain-  
474 modulating spinal interneurons. *J Comp Neurol* 524, 846-873.
- 475 Cheng, L., Duan, B., Huang, T., Zhang, Y., Chen, Y., Britz, O., Garcia-Campmany, L., Ren, X., Vong, L.,  
476 Lowell, B.B., *et al.* (2017). Identification of spinal circuits involved in touch-evoked dynamic  
477 mechanical pain. *Nat Neurosci* 20, 804-814.
- 478 Connor, J.A., and Stevens, C.F. (1971a). Inward and delayed outward membrane currents in isolated  
479 neural somata under voltage clamp. *J Physiol* 213, 1-19.
- 480 Connor, J.A., and Stevens, C.F. (1971b). Voltage clamp studies of a transient outward membrane  
481 current in gastropod neural somata. *J Physiol* 213, 21-30.
- 482 Cui, L., Kim, Y.R., Kim, H.Y., Lee, S.C., Shin, H.S., Szabo, G., Erdelyi, F., Kim, J., and Kim, S.J. (2011).  
483 Modulation of synaptic transmission from primary afferents to spinal substantia gelatinosa neurons  
484 by group III mGluRs in GAD65-EGFP transgenic mice. *J Neurophysiol* 105, 1102-1111.
- 485 Cui, L., Miao, X., Liang, L., Abdus-Saboor, I., Olson, W., Fleming, M.S., Ma, M., Tao, Y.X., and Luo, W.  
486 (2016). Identification of Early RET+ Deep Dorsal Spinal Cord Interneurons in Gating Pain. *Neuron* 91,  
487 1413.
- 488 Daniele, C.A., and MacDermott, A.B. (2009). Low-threshold primary afferent drive onto GABAergic  
489 interneurons in the superficial dorsal horn of the mouse. *J Neurosci* 29, 686-695.
- 490 Delfini, M.C., Mantilleri, A., Gaillard, S., Hao, J., Reynders, A., Malapert, P., Alonso, S., Francois, A.,  
491 Barrere, C., Seal, R., *et al.* (2013). TFAA4, a chemokine-like protein, modulates injury-induced  
492 mechanical and chemical pain hypersensitivity in mice. *Cell reports* 5, 378-388.

493 Duan, B., Cheng, L., Bourane, S., Britz, O., Padilla, C., Garcia-Campmany, L., Krashes, M., Knowlton,  
494 W., Velasquez, T., Ren, X., *et al.* (2014). Identification of spinal circuits transmitting and gating  
495 mechanical pain. *Cell* 159, 1417-1432.

496 Edwards, L., Nashmi, R., Jones, O., Backx, P., Ackerley, C., Becker, L., and Fehlings, M.G. (2002).  
497 Upregulation of Kv 1.4 protein and gene expression after chronic spinal cord injury. *J Comp Neurol*  
498 443, 154-167.

499 Fernandez-Velasco, M., Ruiz-Hurtado, G., Hurtado, O., Moro, M.A., and Delgado, C. (2007). TNF-alpha  
500 downregulates transient outward potassium current in rat ventricular myocytes through iNOS  
501 overexpression and oxidant species generation. *Am J Physiol Heart Circ Physiol* 293, H238-245.

502 Gomez, R., Nunez, L., Vaquero, M., Amoros, I., Barana, A., de Prada, T., Macaya, C., Maroto, L.,  
503 Rodriguez, E., Caballero, R., *et al.* (2008). Nitric oxide inhibits Kv4.3 and human cardiac transient  
504 outward potassium current (Ito1). *Cardiovasc Res* 80, 375-384.

505 Grace, P.M., Gaudet, A.D., Staikopoulos, V., Maier, S.F., Hutchinson, M.R., Salvemini, D., and Watkins,  
506 L.R. (2016). Nitroxidative Signaling Mechanisms in Pathological Pain. *Trends Neurosci* 39, 862-879.

507 Haring, M., Zeisel, A., Hochgerner, H., Rinwa, P., Jakobsson, J.E.T., Lonnerberg, P., La Manno, G.,  
508 Sharma, N., Borgius, L., Kiehn, O., *et al.* (2018). Neuronal atlas of the dorsal horn defines its  
509 architecture and links sensory input to transcriptional cell types. *Nat Neurosci* 21, 869-880.

510 Harris, B.M., Hughes, D.I., Bolton, P.S., Tadros, M.A., Callister, R.J., and Graham, B.A. (2014).  
511 Contrasting alterations to synaptic and intrinsic properties in upper-cervical superficial dorsal horn  
512 neurons following acute neck muscle inflammation. *Mol Pain* 10, 25.

513 Hoeffel, G., Debroas, G., Roger, A., Rossignol, R., Gouilly, J., Laprie, C., Chasson, L., Barbon, P.V.,  
514 Balsamo, A., Reynders, A., *et al.* (2021). Sensory neuron-derived TFAA4 promotes macrophage tissue  
515 repair functions. *Nature* 594, 94-99.

516 Hu, H.J., Carrasquillo, Y., Karim, F., Jung, W.E., Nerbonne, J.M., Schwarz, T.L., and Gereau, R.W.t.  
517 (2006). The kv4.2 potassium channel subunit is required for pain plasticity. *Neuron* 50, 89-100.

518 Hu, H.J., and Gereau, R.W.t. (2003). ERK integrates PKA and PKC signaling in superficial dorsal horn  
519 neurons. II. Modulation of neuronal excitability. *J Neurophysiol* 90, 1680-1688.

520 Hu, H.J., and Gereau, R.W.t. (2011). Metabotropic glutamate receptor 5 regulates excitability and  
521 Kv4.2-containing K(+) channels primarily in excitatory neurons of the spinal dorsal horn. *J*  
522 *Neurophysiol* 105, 3010-3021.

523 Hu, H.J., Glauner, K.S., and Gereau, R.W.t. (2003). ERK integrates PKA and PKC signaling in superficial  
524 dorsal horn neurons. I. Modulation of A-type K+ currents. *J Neurophysiol* 90, 1671-1679.

525 Huang, H.Y., Cheng, J.K., Shih, Y.H., Chen, P.H., Wang, C.L., and Tsaur, M.L. (2005). Expression of A-  
526 type K channel alpha subunits Kv 4.2 and Kv 4.3 in rat spinal lamina II excitatory interneurons and  
527 colocalization with pain-modulating molecules. *Eur J Neurosci* 22, 1149-1157.

528 Hughes, D.I., Sikander, S., Kinnon, C.M., Boyle, K.A., Watanabe, M., Callister, R.J., and Graham, B.A.  
529 (2012). Morphological, neurochemical and electrophysiological features of parvalbumin-expressing  
530 cells: a likely source of axo-axonic inputs in the mouse spinal dorsal horn. *J Physiol* 590, 3927-3951.

531 Jerng, H.H., and Pfaffinger, P.J. (2014a). Modulatory mechanisms and multiple functions of  
532 somatodendritic A-type K (+) channel auxiliary subunits. *Front Cell Neurosci* 8, 82.

533 Jerng, H.H., and Pfaffinger, P.J. (2014b). S-glutathionylation of an auxiliary subunit confers redox  
534 sensitivity to Kv4 channel inactivation. *PLoS One* 9, e93315.

535 Jerng, H.H., Pfaffinger, P.J., and Covarrubias, M. (2004). Molecular physiology and modulation of  
536 somatodendritic A-type potassium channels. *Mol Cell Neurosci* 27, 343-369.

537 Johnston, J. (2021). Pharmacology of A-Type K(+) Channels. *Handb Exp Pharmacol* 267, 167-183.

538 Kuboyama, K., Tsuda, M., Tsutsui, M., Toyohara, Y., Tozaki-Saitoh, H., Shimokawa, H., Yanagihara, N.,  
539 and Inoue, K. (2011). Reduced spinal microglial activation and neuropathic pain after nerve injury in  
540 mice lacking all three nitric oxide synthases. *Mol Pain* 7, 50.

541 Kumamoto, E. (2019). Cellular Mechanisms for Antinociception Produced by Oxytocin and Orexins in  
542 the Rat Spinal Lamina II-Comparison with Those of Other Endogenous Pain Modulators.  
543 *Pharmaceuticals (Basel)* 12, 136.

544 Melzack, R., and Wall, P.D. (1965). Pain mechanisms: a new theory. *Science* 150, 971-979.

545 Mitra, P., and Brownstone, R.M. (2012). An in vitro spinal cord slice preparation for recording from  
546 lumbar motoneurons of the adult mouse. *J Neurophysiol* 107, 728-741.

547 Moehring, F., Halder, P., Seal, R.P., and Stucky, C.L. (2018). Uncovering the Cells and Circuits of Touch  
548 in Normal and Pathological Settings. *Neuron* 100, 349-360.

549 Nowak, A., Mathieson, H.R., Chapman, R.J., Janzso, G., Yanagawa, Y., Obata, K., Szabo, G., and King,  
550 A.E. (2011). Kv3.1b and Kv3.3 channel subunit expression in murine spinal dorsal horn GABAergic  
551 interneurons. *J Chem Neuroanat* 42, 30-38.

552 Olausson, H., Wessberg, J., Morrison, I., McGlone, F., and Vallbo, A. (2010). The neurophysiology of  
553 unmyelinated tactile afferents. *Neurosci Biobehav Rev* 34, 185-191.

554 Oliva, A.A., Jr., Jiang, M., Lam, T., Smith, K.L., and Swann, J.W. (2000). Novel hippocampal  
555 interneuronal subtypes identified using transgenic mice that express green fluorescent protein in  
556 GABAergic interneurons. *J Neurosci* 20, 3354-3368.

557 Peirs, C., and Seal, R.P. (2016). Neural circuits for pain: Recent advances and current views. *Science*  
558 354, 578-584.

559 Petitjean, H., Pawlowski, S.A., Fraine, S.L., Sharif, B., Hamad, D., Fatima, T., Berg, J., Brown, C.M., Jan,  
560 L.Y., Ribeiro-da-Silva, A., *et al.* (2015). Dorsal Horn Parvalbumin Neurons Are Gate-Keepers of Touch-  
561 Evoked Pain after Nerve Injury. *Cell Rep* 13, 1246-1257.

562 Pires da Silva, M., de Almeida Moraes, D.J., Mecawi, A.S., Rodrigues, J.A., and Varanda, W.A. (2016).  
563 Nitric Oxide Modulates HCN Channels in Magnocellular Neurons of the Supraoptic Nucleus of Rats by  
564 an S-Nitrosylation-Dependent Mechanism. *J Neurosci* 36, 11320-11330.

565 Pongs, O., and Schwarz, J.R. (2010). Ancillary subunits associated with voltage-dependent K+  
566 channels. *Physiol Rev* 90, 755-796.

567 Punnakkal, P., von Schoultz, C., Haenraets, K., Wildner, H., and Zeilhofer, H.U. (2014). Morphological,  
568 biophysical and synaptic properties of glutamatergic neurons of the mouse spinal dorsal horn. *J*  
569 *Physiol* 592, 759-776.

570 Seal, R.P., Wang, X., Guan, Y., Raja, S.N., Woodbury, C.J., Basbaum, A.I., and Edwards, R.H. (2009).  
571 Injury-induced mechanical hypersensitivity requires C-low threshold mechanoreceptors. *Nature* 462,  
572 651-655.

573 Strube, C., Saliba, L., Moubarak, E., Penalba, V., Martin-Eauclaire, M.F., Tell, F., and Clerc, N. (2015).  
574 Kv4 channels underlie A-currents with highly variable inactivation time courses but homogeneous  
575 other gating properties in the nucleus tractus solitarii. *Pflugers Arch* 467, 789-803.

576 Tamamaki, N., Yanagawa, Y., Tomioka, R., Miyazaki, J., Obata, K., and Kaneko, T. (2003). Green  
577 fluorescent protein expression and colocalization with calretinin, parvalbumin, and somatostatin in  
578 the GAD67-GFP knock-in mouse. *J Comp Neurol* 467, 60-79.

579 Todd, A.J. (2010). Neuronal circuitry for pain processing in the dorsal horn. *Nat Rev Neurosci* 11, 823-  
580 836.

581 Tsantoulas, C., and McMahon, S.B. (2014). Opening paths to novel analgesics: the role of potassium  
582 channels in chronic pain. *Trends Neurosci* 37, 146-158.

583 Wrobel, L., Schorscher-Petcu, A., Dupre, A., Yoshida, M., Nishimori, K., and Tribollet, E. (2011).  
584 Distribution and identity of neurons expressing the oxytocin receptor in the mouse spinal cord.  
585 *Neurosci Lett* 495, 49-54.

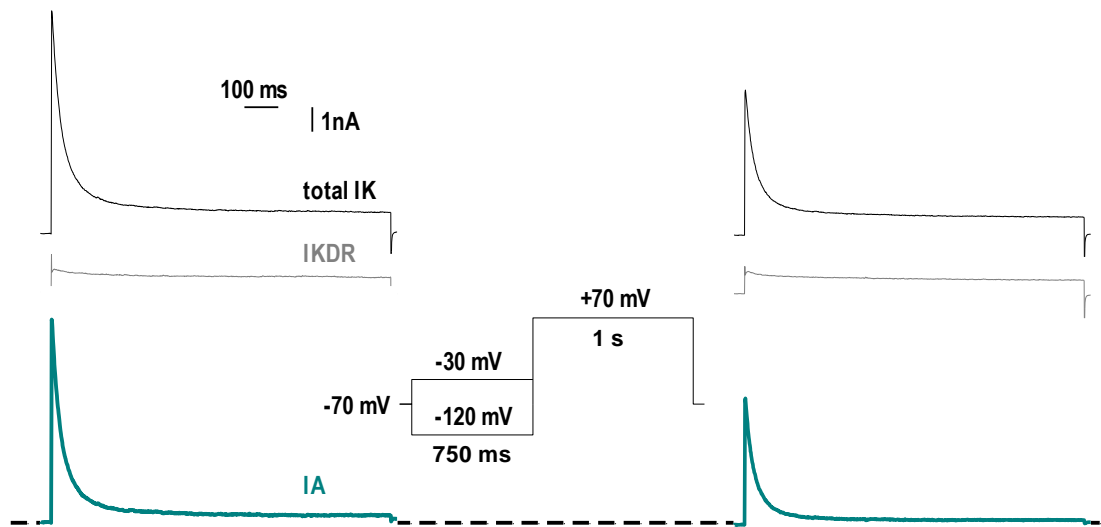
586 Yoo, S., Santos, C., Reynders, A., Marics, I., Malapert, P., Gaillard, S., Charron, A., Ugolini, S.,  
587 Rossignol, R., El Khallouqi, A., *et al.* (2021). TFAFA4 relieves injury-induced mechanical hypersensitivity  
588 through LDL receptors and modulation of spinal A-type K(+) current. *Cell reports* 37, 109884.

589 Zemel, B.M., Ritter, D.M., Covarrubias, M., and Muqem, T. (2018). A-Type KV Channels in Dorsal  
590 Root Ganglion Neurons: Diversity, Function, and Dysfunction. *Front Mol Neurosci* 11, 253.

591 Zhang, H., and Dougherty, P.M. (2011). Acute inhibition of signalling phenotype of spinal GABAergic  
592 neurons by tumour necrosis factor-alpha. *J Physiol* 589, 4511-4526.

593 Zhang, Y., Liu, S., Zhang, Y.Q., Goulding, M., Wang, Y.Q., and Ma, Q. (2018). Timing Mechanisms  
594 Underlying Gate Control by Feedforward Inhibition. *Neuron* 99, 941-955 e944.

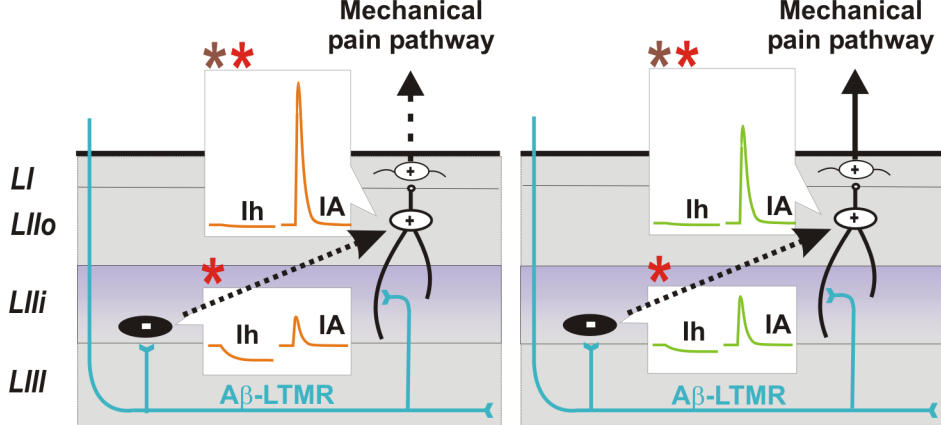
595



GAD67-GFP- (excitatory) interneuron



GAD67-GFP+ (inhibitory) interneuron



**Control conditions**  
**Normal mechanosensation**

**Ipsilateral to nerve lesion**  
**Mechanical hypersensitivity**

**Table 1: Toolbox for recording IA in spinal cord slices**

Goal	Methodological trick	References
Good slices	Rapid removal of the spinal cord to prevent anoxia; fast intracardiac perfusion with adequately oxygenated slicing solution	Mitra & Browstone 2012 Yoo et al. 2021 (methods)
Access resistance ( $R_a$ ; between the pipette and the cell) as low as possible	Reducing $R_a$ to obtain values $< 20 \text{ M}\Omega$ by using recording pipettes with tips as large as possible; fire-polishing helps	Strube et al. 2015 (Fig. 4)
IA resolution & isolation (1)	Pharmacological identification of the Kv family carrying the IA	Johnston 2021 Strube et al. 2015
IA resolution & isolation (2)	Determination of at least $V_{1/2}$ inactivation to identify the most appropriate hyperpolarizing potential for the conditioning prepulse	
IA resolution & isolation (3)	If not wishing to study the IA carried by Kv3.3 or Kv3.4, decrease the persistent IK ( $I_{K_{DR}^*}$ ) with high [TEA] in the recording solution.	Strube et al. 2015 (Fig. 4) Yao et al. 2013 (methods)
IA resolution & isolation (4)	P/N subtraction method to eliminate the effects of leak current on whole-cell responses (but requires a longer recording time)	Melnick 2011 (methods)
IA resolution & isolation (5)	Obtain the difference current ( $I_{K_{total}} - I_{K_{DR}}$ ) by subtracting the full current traces. Subtracting the maximum $I_{K_{DR}}$ from the total instantaneous IK would lead to: 1- Underestimation of IA amplitude (because $I_{K_{DR}}$ is activated more slowly than IA) 2- An impossibility of inactivation time course evaluation	Hess & El Manira 2001 (Fig.1) Luther & Tasker 2000 (Fig. 2A) Strube et al. 2015 (discussion)
Targeting the spinal area affected by a peripheral lesion	The SNI model, for example, can be used to target the site at which LIIi and LIIo interneurons should be patched with precision, as this injury circumscribes the activation of microglia	Yoo et al. 2021 (methods)

- \*  $I_{K_{DR}}$ : delayed rectifier  $K^+$  current

**Table 2: Comparison of IA densities in LII excitatory and inhibitory interneurons in slices from mice either naïve or subjected to SNI (data from Yoo et al. 2021)**

Location	Neuron type	<i>n</i>	Mouse model	IA density (+70 mV; pA/pF)	Ih density (-120 mV; pA/pF)
LII outer	ExIN	46	NAIVE	<b>295</b>	-2
		26	SNI	<b>192 (35% decrease)</b>	-2
	InhIN	25	NAIVE	95	-2
		14	SNI	84	-1.5
LII inner	ExIN	28	NAIVE	258	-2
		21	SNI	245	-22
	InhIN	52	NAIVE	<b>42</b>	<b>-112</b>
		32	SNI	<b>73 (74% increase)</b>	<b>-6</b>